

## Structural Performance Analysis Of Steel Bridge In Lempake, Samarinda City Using Finite Element Method

Wahyu Mahendra Trias Atmadja, Habir, Maraden Panjaitan

Lecturer of the Faculty of Civil Engineering, University of 17 Agustus 1945 Samarinda,  
Ir. H. Juanda Street, No.80, Samarinda, Province of East Kalimantan, Indonesia

### ABSTRACT

This research aims to analyze the structural performance of steel bridges under various load conditions, focusing on the bridge located in Samarinda. The main objective is to evaluate the strength and stability of the bridge's structural components, particularly the steel girders, using finite element analysis (FEA). The methodology involves conducting a detailed structural analysis, referencing relevant standards such as SNI 1725:2016 and SNI 1729:2015, as well as international steel construction guidelines. Field data were collected to assess the existing conditions of the bridge, and the material properties were derived from SM490 steel specifications. The analysis also considers different load types, including dead loads, live loads, and environmental factors such as wind. The results show that the steel girders perform well under the specified load conditions, maintaining structural integrity and safety within acceptable limits. However, certain areas of the bridge require reinforcement to improve overall stability. The findings contribute to a better understanding of the bridge's structural behavior and provide recommendations for future maintenance and improvement efforts.

**Keywords:** Steel Bridge, Structural Analysis, Finite Element Analysis, Load Conditions, SM490 Steel.

Received 25 Nov., 2024; Revised 02Dec., 2024; Accepted 04Dec., 2024 © The author(s) 2024.

Published with open access at [www.questjournals.org](http://www.questjournals.org)

### I. INTRODUCTION

The Lempake Tepian Bridge, located in Lempake Village, North Samarinda District, Samarinda City, is a vital piece of infrastructure for the daily transportation needs of the local community. This bridge is a composite type, featuring a main span of 30 meters and a width of 8 meters, connecting both sides of a river approximately 35 meters wide (Sukmawati & Wibowo, 2020). The significance of this bridge lies in its role as a crucial link within the local transportation network, supporting both economic and social activities in the surrounding area (Kurmiawan et al., 2022).

This study focuses on analyzing the superstructure of the Lempake Tepian Bridge using structural analysis software to assess its strength and safety. The analysis includes load assessment and structural evaluation, aiming to determine the adequacy of the steel girders, shear control, and deflection limits of the bridge (Yuliana & Pratama, 2021). By examining these factors, the research seeks to ensure that all structural components meet the required safety standards.

Furthermore, this study identifies the need for manual recalculation of internal forces as an additional measure to verify the accuracy of the analysis results. Errors in steel profile selection or structural calculations can impact the performance and safety of the bridge (Aditya, 2023). Thus, recalculation and verification are crucial for ensuring the long-term reliability and success of the bridge's structural integrity.

### II. MATERIALS AND METHODOLOGY

#### 2.1. Study Location

The study was conducted at the Lempake Tepian Bridge, situated in the North Samarinda District of Samarinda City, East Kalimantan Province, Indonesia. This location is specifically within the Sempaja Utara Sub-District area, which is positioned at the coordinates of Abutment 1: 0°26'19"S 117°10'13"E and Abutment 2: 0°26'18"S 117°10'13"E. The bridge spans a width of approximately 35 meters across the river and features a total length of 30 meters with a width of 8 meters.

The geographical coordinates and dimensions indicate that the bridge serves as a crucial transportation link across the river, connecting areas that are vital for both local commerce and community interactions. The location's specifics, including its exact positioning and structural dimensions, are critical for understanding the bridge's role in the regional infrastructure and for conducting accurate structural analyses.

This area is characterized by its urban environment, with significant daily traffic flow, making the bridge an essential component of the local transportation network. The study location's characteristics, including the river width and the bridge's span, are key factors in the assessment and analysis of the bridge's structural integrity and load-bearing capacity.

**2.2. Data**

Table 1 details structural data for a bridge with a total length of 30 meters and a width of 10 meters. The bridge's deck is supported by a slab with a thickness of 0.22 meters, ensuring adequate strength and durability for vehicular loads. An asphalt layer, 0.10 meters thick, is applied on top of the slab to provide a smooth driving surface while enhancing protection against wear and weather conditions.

**Table 1.** Structural Data

No.	Structural Data	Dimension (m)
1.	Bridge Length	30.00
2.	Bridge Width	10.00
3.	Bridge Slab Thickness	0.22
4.	Asphalt Layer Thickness	0.10
5.	Rainwater Ponding Depth	0.05

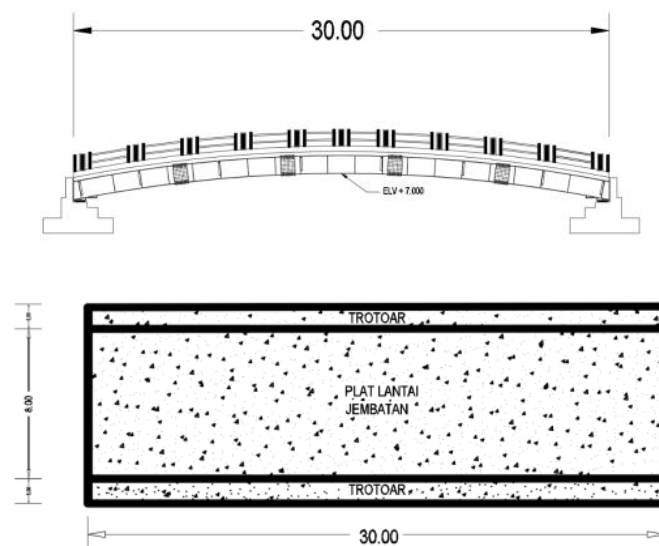


**Fig. 1.** View of the Bridge

In addition to the structural layers, the bridge design accounts for a rainwater ponding depth of 0.05 meters, which is crucial for managing surface water during heavy rainfall. This feature ensures that the bridge maintains proper drainage, preventing potential hazards such as hydroplaning or excessive water accumulation. These dimensions reflect a well-balanced approach to structural integrity and safety for both the bridge and its users.

**2.3. Data Analysis Techniques**

In this research, data analysis is performed using a quantitative approach involving load analysis, superstructure analysis, moment control, shear control, deflection control, and connection analysis. These analyses are conducted using structural analysis software that supports finite element simulation. Below are the steps along with the related formulas:

**2.3.1. Load Analysis**

Load analysis is conducted to determine the maximum load acting on the bridge structure, including live loads (LL), dead loads (DL), wind loads (WL), and vehicle loads. These loads are calculated according to bridge loading regulations (SNI 1725:2016).

Load Formula:

$$W_{total} = W_{DL} + W_{LL} + W_{WL} + W_{veh}$$

Information:

- $W_{total}$  = total load
- $W_{DL}$  = dead load
- $W_{LL}$  = live load
- $W_{WL}$  = wind load
- $W_{veh}$  = vehicle load

### 2.3.2. Structural analysis

Structural analysis is performed to evaluate the structure's response to the applied loads, including moment, shear, and deflection analysis. The software will simulate the behavior using the finite element method to calculate internal forces on Hibbeler, R.C. (2017).

Bending Moment Formula:

$$M = \frac{W \cdot L^2}{8}$$

Information:

- $M$  = bending moment
- $W$  = total load applied to the span
- $L$  = span length of the bridge

### 2.3.3. Bending Moment and Shear Control

Bending moment and shear control are performed to ensure that the steel profile WF 800x300x14x26 used in the longitudinal girder satisfies the bending moment and shear strength criteria according to AISC Steel Construction Manual, 15th Edition:

Bending Moment Control:

$$M_u < \phi M_n$$

Information:

- $M_u$  = applied bending moment
- $M_n$  = nominal bending moment capacity
- $\phi$  = strength reduction factor (typically 0.9)

Swipe Control :

$$V_u < \phi V_n$$

Information:

- $V_u$  = applied shear
- $V_n$  = nominal shear capacity
- $\phi$  = strength reduction factor (typically 0.75)

### 2.3.4. Deflection control

The deflection caused by the loads on the structure is calculated and compared to the maximum allowable deflection. The deflection is calculated using the following formula Gere, J.M. & Timoshenko, S.P. (1997):

Deflection Formula:

$$\delta = \frac{5wL^4}{384EI}$$

Information:

- $\delta$  = maximum deflection
- $w$  = load per unit length
- $L$  = span length
- $E$  = modulus of elasticity
- $I$  = moment of inertia of the section

### 2.3.5. Connection analysis

Connection analysis is performed to calculate the strength of bolt connections in the girder, considering both shear and bearing forces on the bolts according to SNI 1729:2015.

Bolt connection formula:

$$P_{allow} = n \cdot P_{bolt}$$

Information:

- $P_{allow}$  = allowable connection capacity
- $n$  = number of bolts
- $P_{bolt}$  = capacity of one bolt against shear or bearing

Using these data analysis techniques, the field survey and secondary data will be processed to evaluate the structural condition of the bridge comprehensively, both in terms of strength and structural reliability.

### III. RESULTS AND DISCUSSION

A summary of load results and their corresponding units for bridge design is presented in Table 2.

**Table 2.**Summary of Load Results and Their Corresponding Units for Bridge Design

Load Type	Load Result	Unit
<b>1. Structural Dead Load (MS)</b>	63.155	kN/m
<b>2. Additional Dead Load (MA)</b>		
Handrail	0.500	kN/m
Trotoar	7.920	kN/m
Rainwater Load	0.736	kN/m <sup>2</sup>
Asphalt Layer	1.650	kN/m <sup>2</sup>
<b>3. Traffic Load (TD)</b>		
Uniform Beam Load	13.5	kN/m
Concentrated Line Load	231	kN/m
Beban Merata Balok	280	kN/m
<b>4. Braking Force (TB)</b>	56.250	kN/m
<b>5. Pedestrian Load (TP)</b>	3.750	kN/m
<b>6. Wind Load (EW)</b>	3.491	kN/m
<b>7. Temperature Load (Temp)</b>	30	°C

#### 3.1. Bridge Structure Analysis

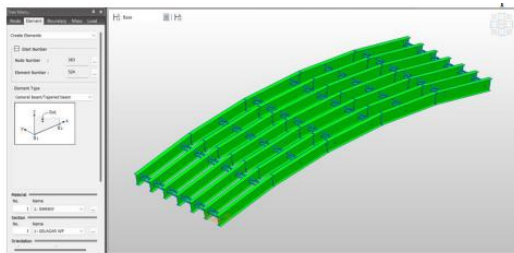


**Fig 2.**The Bridge Modeling

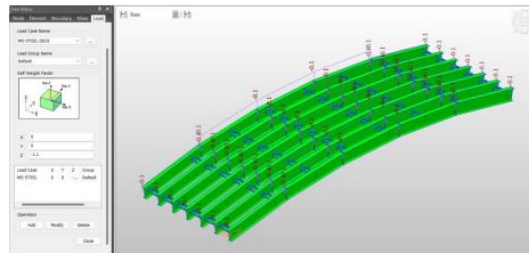


**Fig 3.** The Load Modeling on the Girders

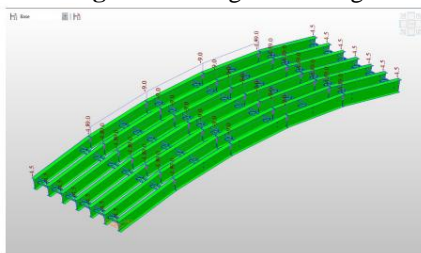


**Fig 4.**The Load Modeling of the Vehicle Floor Slab

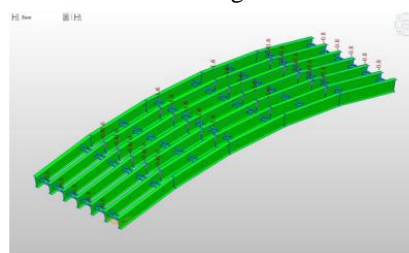


**Fig 5.**The Load Distribution on a Bridge

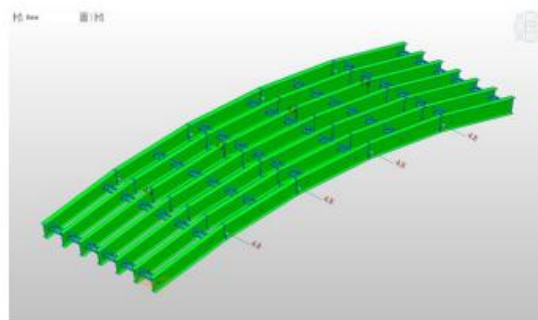


**Fig. 6.** The Wind Load Distribution on the Bridge Structure

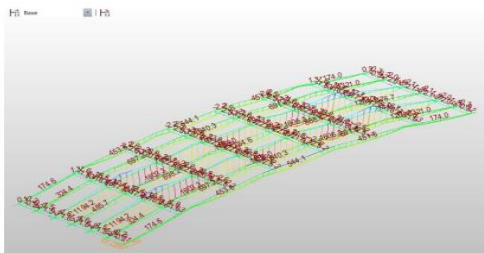
Based on the bridge modeling shown in Figure 2, the bridge beam structure has been designed using finite elements, with element and node numbering automatically generated by the structural analysis software. The elements used are the General Frame (Beam) type, which is commonly employed to model long beams subjected to bending loads, with the material being steel (S355JR), by standard bridge materials. The modeling input includes 363 nodes and 360 elements, indicating a level of detail sufficient for analyzing the bridge's response to loads. The model illustrates the distribution of forces and deformations along the beam elements, with the orderly element numbering providing a clear depiction of how the load will be distributed throughout the bridge structure.

Based on the load modeling on the girders, the bridge is analyzed under uniformly distributed loads along the beam elements. The load case applied is a dead load with steel material (HS STEEL S355), and a load factor of 1.2, indicating that the dead load is applied under standard design conditions. The loads are distributed across all girder elements, with forces proportionally applied based on the structural configuration of the bridge. This result in Figure 3 illustrates the response of the girder elements to the applied load, which is evenly distributed through the primary elements. This balanced load distribution is crucial to avoid stress concentrations that could lead to excessive deformations or structural failure.

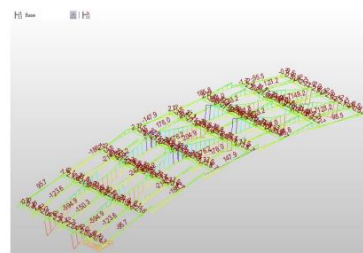
Based on the load modeling Figure 4 of the vehicle floor slab, the bridge is analyzed with a uniformly distributed load across the floor slab, which is a critical component in supporting vehicular traffic. This load represents the distribution of the weight of vehicles passing over the bridge, with forces applied to the slab elements. Each slab element receives proportional forces based on its placement within the overall structure. The load distribution shown in the figure is essential to ensure that the floor slab can withstand the pressure generated by traffic loads, preventing localized deformation or structural damage.

Figure 5 displays the load distribution on a bridge with multiple lanes, each subjected to different load conditions. The load application appears uniform across the bridge girders, which indicates that the structural model effectively captures the load transfer mechanism. In the results, the applied lane loads are visualized as discrete forces along the girders, reflecting real-world loading conditions such as traffic or environmental forces. The variation in load intensity along the span could point to areas of higher stress concentration, which are critical for the structural integrity of the bridge.

Figure 6 shows the wind load distribution on the bridge structure, concentrated at several points along the bridge span. The wind load is applied uniformly to the main structural elements, such as the longitudinal girders, indicating how wind forces affect the lateral stability of the bridge. In the results, this wind load distribution suggests how wind pressure induces lateral forces on the bridge, especially in open areas that are more exposed to wind forces.



**Fig. 7.** The YZ Moment Distribution



**Fig 8.** The YZ Shear Distribution

Figure 7 presents the YZ moment distribution along the bridge structure. The moment diagram appears to highlight areas of higher bending moments at specific locations, likely due to load concentrations and structural supports. In the results, the moments are predominantly observed along the girders and crossbeams, which indicates that these elements are experiencing significant bending forces. These moments are critical to structural integrity as they represent the stresses that could lead to deflection or even failure if not properly accounted for.

Figure 8 appears to display a structural analysis of a shear force diagram along the YZ plane for a bridge or similar structure. In the results and discussion section, it is important to focus on the critical points observed in the diagram. The variation of shear forces across the structure can indicate the stress distribution, especially around joints and supports where forces tend to concentrate. Higher values at specific locations may suggest the need for reinforcement or attention in design adjustments. The uniformity of the shear force distribution across the span also plays a significant role in evaluating the overall structural integrity.

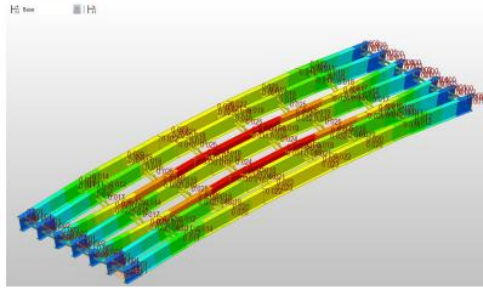


Fig 9. Displacement DXYZ

The DXYZ displacement diagram shows the distribution of displacement across the structure, with color variations indicating the level of displacement at each point. The red color represents the maximum displacement, typically occurring at the mid-span, highlighting the area experiencing the highest load. In contrast, green to blue colors depict lower displacement, indicating more stable regions. This analysis demonstrates that the structure undergoes varying levels of displacement, with high concentrations in certain critical areas (Figure 9).

### 3.2. Control of Steel Girder: Steel Profile: IWF 800.300.14.26

#### 3.2.1. Control Before Composite:

- The maximum moment ( $M_u$ ) adalah **102.68 kNm**.
- The allowable moment before the composite is calculated as follows:

$$M_n = \frac{2}{3} \times f_y \times S_x = 1630.33 \text{ kNm}$$

- After applying the reduction factor ( $\phi = 0.9$ ):  

$$\phi M_n = 0.9 \times 1630.33 = 1467.63 \text{ kNm}$$
- Since  $M_u = 102.68 \text{ kNm} < \phi M_n = 1467.63 \text{ kNm}$ , this result is **OK**.

#### 3.2.2. Shear Control:

- The shear force after the composite ( $V_u$ ) = **112.58 kN**.
- The height-to-thickness ratio is:

$$\frac{h}{tw} = \frac{800}{14} = 57.14 < 1100 \times \sqrt{335} = 60.09$$

Therefore, the shear force is calculated as:

$$V_n = 0.6 \times f_y \times h \times tw = 0.6 \times 335 \times 800 \times 14 = 225.12 \text{ kN}$$

- After applying the reduction factor ( $\phi = 0.9$ ):  

$$\phi V_n = 0.9 \times 225.12 = 202.61 \text{ kN}$$
- Since  $V_u = 112.58 \text{ kN} < \phi V_n = 202.61 \text{ kN}$ , this result is **OK**.

#### 3.2.3. Bending Moment Control with Lateral Buckling:

- The span length ( $L_b$ ) = **150 cm**.
- The critical length ( $L_p$ ):  

$$L_p = 1.76 \times i_y \times E f_y = 8625212290.90 \text{ cm}$$
- The allowable bending moment:  

$$M_n = f_y \times S_x = 335 \times 7300 = 24455 \text{ kNm}$$
- After applying the reduction factor ( $\phi = 0.9$ ):  

$$\phi M_n = 0.9 \times 24455 = 22009.50 \text{ kNm}$$
- Since  $M_u = 1344.4 \text{ kNm} < \phi M_n = 22009.50 \text{ kNm}$ , this result is **OK**.

#### 3.2.4. Deflection Control:

- Modulus of elasticity ratio:

$$n = \frac{E_s}{E_c} = \frac{200000}{25310} = 7.90$$

- Transformed concrete area:

$$A_c = \frac{b_{eff} \times t_p}{n} = \frac{8000 \times 220}{7.90} = 222730 \text{ mm}^2$$

- Neutral axis( $y_a$ ):

$$y_a = \frac{A_c \times (\frac{t_p}{2}) + A_s \times (t_p + \frac{d}{2})}{A_c + A_s} = 309.35 \text{ mm}$$

- Composite moment of inertia:

$$I_{komposit} = 292000 + 26800 \times \left(220 + \frac{1000}{2} - 309.535\right)^2 + \frac{1}{12} \times 205.6 \times 2203 + 41762 \times (309.353 - 2002)^2$$

- Deflection due to live load:

$$\delta = 5384 \times \frac{3.5 \times 30000^4}{200000 \times 6532410691.62} + 148 \times 13500 \times 300003200000 \times 6532410691.62 = 34.067 \text{ mm}$$

- Deflection due to concentrated load T:

$$\delta = \frac{1}{48} \times 56000 \times 300003200000 \times 6532410691.62 = 24.11 \text{ mm}$$

- Allowable deflection:

$$\delta_{ijin} = L800 = 30000800 = 37.5 \text{ mm}$$

### 3.2.5. Connection Calculation:

- Connection plate type: **SM490**,  $F_y = 240 \text{ Mpa}$ ,  $F_u = 370 \text{ Mpa}$ ,  $F_{ubolts} = 620 \text{ Mpa}$ .
- Bolt diameter = **25.4 mm**, tolerance = **3.2 mm**, plate thickness = **20 mm**, plate width = **700 mm**.
- Yield strength of the connection:

$$Resistance = 30240000 \text{ N}$$

- Fracture resistance:

$$Resistance = 26329200 \text{ N} > 2251200 \text{ N (OK)}$$

- Number of bolts: **49 bolts**, bolt bearing strength: **33.97 tons/bolt**, shear strength: **18.63 tons/bolt**.

- Total bolt resistance:

$$T_n = 8947648.6 \text{ N} > 2251200 \text{ N (OK)}$$

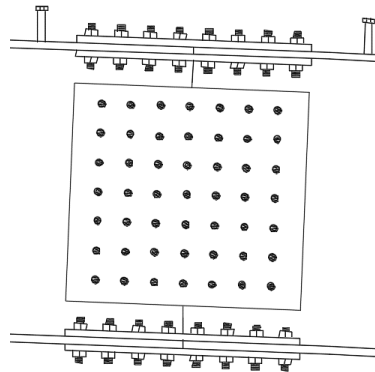


**Fig 10.**The Connections using SM490 Plates and 25.4 mm Diameter Bolts

Based on the control calculations for the steel girder IWF 800.300.14.26, the bending moment, shear, and lateral buckling criteria show that the structure can safely withstand the applied loads according to the design values. The moments experienced by the structure are below the allowable limits, with a shear ratio and bending moment that meet the design criteria. The deflection caused by live loads and concentrated loads is also within the allowable deflection limit, ensuring that the structure does not experience significant deformation. The connections using SM490 plates and 25.4 mm diameter bolts are adequate, with a sufficient number of bolts to withstand both shear and bearing forces. Overall, the steel girder and connections meet the safety and structural performance criteria as expected (Figure 10).

### 3.2.6. Vehicle Floor Slab Design

Longitudinal and Transverse Reinforcement:

- Longitudinal reinforcement: D16 – 150 mm (cross-sectional area: **1843 mm<sup>2</sup>**).
- Transverse reinforcement: D16 – 150 mm (cross-sectional area: **1843 mm<sup>2</sup>**).

Shear Force Control for the Slab:

- Shear force ( $V_u$ ) must be checked to ensure that it is below the concrete shear capacity ( $\phi V_c$ ):

$$V_u = T_u = 263.25 \text{ kN} < \phi V_c = 0.75 \times 418 \text{ kN} = 313 \text{ kN (OK)}$$

This shows that the applied shear force is less than the allowable shear capacity of the slab, meaning the design is within safe limits.

### 3.2.7. Bearing Design

The bearing used is an **elastomeric bearing** with dimensions **665 x 665 mm<sup>2</sup>**. The following checks were performed :

**Control of Shape Factor(S):**

- The shape factor ( $S$ ) is calculated as:

$$S = \frac{A}{p \cdot t_e} = \frac{409575}{2 \cdot (645 + 635) \cdot 15} = 10.67S$$

- The shape factor must meet the requirement of **4 < S < 12**, which it does, indicating that the bearing's dimensions are within acceptable limits for safe performance (OK).

**Bearing Design Requirements:**

- The requirement for maximum horizontal displacement ( $H'$ ) is calculated as:

$$H' \leq 0.1 \times (V_{max} + 3 \cdot A_{eff} \cdot 0.001)$$

- o  $H' \leq 17.63 \text{ kN}$
- o  $0.1 \times (357.452 + 3 \times 405744.08 \times 0.001) = 157.42 \text{ kN}$
- o  $17.63 \text{ kN} < 157.42 \text{ kN (OK)}$

In the design of the vehicle floor slab, both the longitudinal and transverse reinforcement (D16-150) provide adequate strength to support the applied loads. The shear force control shows that the actual shear force experienced by the slab is lower than the allowable capacity, ensuring that the slab will not fail under typical loading conditions.

For the bearing design, the elastomeric bearing with dimensions 665 x 665 mm<sup>2</sup> satisfies the shape factor requirement, confirming that the bearing's proportions are within safe operating limits. Additionally, the bearing's maximum horizontal displacement meets the safety requirements, indicating that it can accommodate the loads without excessive deformation. Overall, the vehicle floor slab and the elastomeric bearing design are structurally sound and meet all necessary safety standards.

## IV. CONCLUSION

Based on the analysis conducted on the Lempake Tepian Bridge in North Samarinda District, several conclusions can be drawn regarding the bridge's structural performance, loading capacity, and the efficiency of its elements. The loading analysis indicates that the bridge can withstand various loads, including dead loads, live loads, traffic loads, wind loads, and vehicle loads by the SNI 1725:2016 standard. The additional loads from handrails, sidewalks, rainwater, and asphalt layers contribute significantly to the total load. The bending moment and shear force analysis reveal that the WF 800x300x14x26 steel profiles used in the longitudinal girders meet the criteria for flexural strength and shear stress based on the AISC Steel Construction Manual. Moreover, the deflection analysis shows that the displacements caused by distributed loads are within the allowable limits as per SNI standards, ensuring the bridge's structural integrity under normal operations.

The performance of the connections is adequate, with bolted joints meeting the SNI 1729:2015 standards, and capable of withstanding shear and bearing forces. The bridge also demonstrates good stability against wind loads, with wind forces distributed evenly across the main structural elements, preventing significant deformation. Dynamic loads from vehicular traffic are well-distributed across the bridge span, ensuring balanced load distribution. The maximum displacement observed, at 0.021 meters, remains within safe limits, with no indication of structural failure. In conclusion, the Lempake Tepian Bridge is structurally sound and safe for use, although regular monitoring and inspections are recommended to maintain optimal performance and address any potential long-term environmental or load-related changes.

## REFERENCES

- [1]. Demers, A.M. (2002). Sediment Accumulation and its Impact on Reservoir Capacity. *Water Resources Research*, 38(3): 1127-1134
- [2]. Garmin. (n.d.). Garmin GPSMAP 585Plus User Manual. Retrieved from Garmin Website
- [3]. Laporan Pengerukan Sedimentasi Bendungan Benanga, Samarinda. Jakarta: Balai Wilayah Sungai Kalimantan IV
- [4]. Liana, U.W.M., Santoso, T., & Yudhistira, A. (2023). Analisis Penyusutan Kapasitas Bendungan Benanga Akibat Sedimentasi. *Journal of Water Resources Management*, 15(3): 215-230
- [5]. Ministry of Public Works and Public Housing, Directorate General of Water Resources. (2021)



- [6]. Nur, A., Hatta, M. P., Thaha, M.A., and Surimihardja, D.A (2019). Preliminary Modelling of Characteristics of Current and Batimetry in The Confluence of Mahakam River and Karang Mumus River. *IJESCA*, 6(1): 155-164
- [7]. Poerbandono, S., & Mardiatno, D. (2005). *Survei Batimetri: Teknik Pengukuran dan Aplikasinya*. Yogyakarta: Gadjah Mada University Press
- [8]. Santoso, H. (2015). Impact of Sedimentation on Reservoir Capacity: A Case Study of Benanga Dam. *Indonesian Journal of Environmental Management*, 9(2): 102-115
- [9]. Urick, R.J. (1983). *Principles of Underwater Sound* (3rd ed.). New York: McGraw-Hill